

Droplet Formation in Quark-Gluon Plasma at Low Temperatures and High Densities

R.S. Bhalerao^a and R.K. Bhaduri^b

^a *Department of Theoretical Physics, Tata Institute of Fundamental Research,
Homi Bhabha Road, Colaba, Mumbai 400 005, India*

and

^b *Department of Physics, McMaster University, Hamilton, Ontario L8S 4M1, Canada*

Abstract

Considering the low-temperature (T) and high-baryon-number-density (n_B) region of the QCD phase diagram, we present a model for the first-order phase transition between the quark-gluon plasma (QGP) and the recently proposed colour superconducting phase. We study nucleation of a droplet of the superconducting phase within the metastable QGP gas. Numerical results for the activation energy, radius and other physical parameters of the droplets, at various temperatures, densities and gap parameters, are given. We have estimated the latent heat of the phase transition. In the $T - n_B$ plane, we are able to demarcate the region of the superconducting phase.

PACS numbers: 12.38.Mh, 12.38.Aw, 26.60.+c, 64.60.Qb

Keywords: Quark-gluon plasma, QCD phase transition, colour superconductivity, droplet formation, diquark

E-mail: bhalerao@theory.tifr.res.in, bhaduri@smiley.physics.mcmaster.ca

I. INTRODUCTION

Our understanding of the QCD matter at low temperatures (T) and high baryon number densities (n_B) has developed rapidly over the past few years; for recent reviews, see [1–3]. A likely scenario is that in this region, quarks form Cooper pairs and new condensates develop. One of the most interesting questions today concerns the detailed mapping of the QCD phase diagram, especially in the above region where QCD may exhibit a colour superconducting phase. In this context, the light quark masses ($m_{u,d,s}$) are expected to play an important role. Figure 1 shows two likely scenarios corresponding to $m_s \gg m_{u,d} \neq 0$ and $m_s = m_{u,d} \simeq 0$. The transition between the quark-gluon plasma (QGP) phase and the colour superconducting phase is expected to be first order, in QCD [1,4].

In this paper, we study the first-order phase transition between the QGP phase and the colour superconducting phase (Fig. 1). Our approach is phenomenological and is similar in spirit to that adopted by Côté and Kharchenko [6]. They, however, studied the Bose-Einstein condensation in a gas of trapped atomic hydrogen at temperatures $\sim 50 \mu K$ and densities $\sim 10^{14} \text{ cm}^{-3}$. Temperatures and densities that we shall consider here are, of course, vastly different, and QGP has very little in common with the atomic hydrogen gas. *Interestingly, however, as we shall see, the same physics of activation energy barrier governs the formation of droplets in both cases.*

It is important to get a handle on the cold and dense quark matter because of its possible relevance to the neutron-star core. While the region of *asymptotic* densities is amenable to rigorous calculations, the same cannot be said about the region of *intermediate* densities studied here. Both numerical (lattice) and direct experimental studies of this region of the QCD phase diagram are out of reach at the moment. Hence a phenomenological study such as the present one is appropriate and worthwhile. It has allowed us to make quantitative statements about the schematic phase diagram in Fig. 1.

Alford et al. [7] have discussed droplet formation in the transition between the hadronic matter phase and the 2SC phase (Fig. 1), at $T = 0$, as a function of density. The chiral

symmetry is restored inside their droplets (which they call nucleons) but is broken outside. Neergaard and Madsen [8] also have studied the droplet formation but in the QGP to hadronic matter transition occurring at low baryon number densities. In this paper, we have considered the QGP to colour-superconducting phase transition occurring at high n_B . *To our knowledge, droplet formation in this transition has not been discussed previously in the literature.* Our droplets are the opposite of those in [7] in the sense that the chiral symmetry is broken inside our droplet, but is restored outside.

II. MODEL

Consider a gas of weakly interacting quarks, antiquarks and gluons in a volume V . We take q and \bar{q} to be the massless current quarks (Fig. 1). We are interested in low temperatures (T) and high number densities (n) such that $n\lambda^3 \gg 1$ where λ is the thermal wave length (see Appendix). We also need the baryon number density $n_B = (n_q - n_{\bar{q}})/3$ to be large compared to that for the normal nuclear matter, namely 0.17 fm^{-3} .

If the interactions among the particles are treated to the lowest order in α_s , the strong coupling constant (Fig. 2), the baryon number density is given by ($c = \hbar = 1$)

$$n_B = \left(1 - \frac{2\alpha_s}{\pi}\right) \frac{d_q}{3} \left[\frac{\mu_q(kT)^2}{6} + \frac{\mu_q^3}{6\pi^2} \right], \quad (1)$$

where $d_q = 2 \text{ (spin)} \times 3 \text{ (colour)} \times 3 \text{ (flavour)} = 18$ is the quark degeneracy factor, k is the Boltzmann constant and μ_q is the quark chemical potential [9]. For a given baryon number density n_B and temperature T , Eq. (1) uniquely fixes μ_q . This in turn determines the total energy and pressure of the gas as

$$E_{gas} = \left(1 - \frac{15\alpha_s}{4\pi}\right) d_g V \frac{\pi^2(kT)^4}{30} + d_q V \left[\left(1 - \frac{50\alpha_s}{21\pi}\right) \frac{7\pi^2(kT)^4}{120} + \left(1 - \frac{2\alpha_s}{\pi}\right) \left(\frac{\mu_q^2(kT)^2}{4} + \frac{\mu_q^4}{8\pi^2} \right) \right], \quad (2)$$

$$P_{gas} = E_{gas}/3V. \quad (3)$$

Here $d_g = 2 \text{ (spin)} \times 8 \text{ (colour)} = 16$ is the gluon degeneracy factor. It was possible to obtain the above analytic expressions because we have considered the gas of quarks as well

as antiquarks, rather than a gas of quarks alone [9]. At low T and high n_B , the μ_q terms in the pressure dominate and the gluonic pressure arising from the first term in Eq. (2), is quite negligible.

We now consider the first-order phase transition from QGP to the superconducting phase as the temperature is lowered (Fig. 1). In the latter phase, as a result of the attractive one-gluon-exchange interaction between quarks in the colour $\bar{\mathbf{3}}$ channel, quarks near the Fermi surface tend to pair up as bosons. These are the Cooper pairs which we assume to be massless. Density fluctuations in the metastable QGP gas may provide suitable conditions for nucleation and growth of a droplet of the superconducting phase. The high-temperature phase (QGP) is present around the droplet and the low-temperature superconducting phase exists inside the droplet. We will presently explore the energetics for the formation of such a droplet by calculating the energy barrier between the two phases.

We have given above the expressions for number density, energy and pressure of the QGP; see Eqs. (1)-(3). We now derive corresponding expressions for the superconducting phase inside the droplet. Before we begin, it is necessary to recall important differences between the BCS superconductor and the colour superconductor. (a) In the BCS theory of superconductivity the ratio of the energy gap (Δ) to the Fermi kinetic energy for a typical metal is of the order of 10^{-4} . In contrast, in the problem under consideration, the gap Δ is estimated to vary between several tens of MeV to about 100 MeV [1–3], and the quark chemical potential μ_q appearing in Eq. (1) takes values between ~ 250 and ~ 600 MeV for the n_B and T considered here. (b) In the BCS superconductor, the Debye energy ω_D is much smaller than the chemical potential μ , while in the colour superconductor, the two may be of the same order of magnitude. (c) Finally, if n is the density of electrons and ξ the Pippard coherence length which measures the spatial extension of the Cooper pair wave function, then in the BCS theory, $n\xi^3 \gg 1$. In the present case, on the other hand, $\xi \simeq 1/(\pi\Delta) \simeq 0.6$ fm for $\Delta = 100$ MeV, and $n\xi^3 < 1$ for the densities considered in this paper. This suggests that the qq pairs are rather compact objects unlike Cooper pairs of electrons in a metal. For a good discussion of these and related issues, see a review article by Kerbikov [10]. We shall

make use of the above points while deriving expressions for thermodynamics quantities of the droplet. For the sake of simplicity, we shall assume that all quarks in the energy interval $(\mu_q - \Delta, \mu_q)$ form Cooper pairs and all other quarks remain unpaired, and shall ignore other interactions.

Consider a spherical region of radius R_d , volume V_d , containing N_1 quarks out of which N_2 remain unpaired and N_3 undergo Cooper pairing, when the pairing interaction is “switched on”. We have

$$N_1 = \frac{d_q V_d}{(2\pi)^3} \int_0^\infty 4\pi p^2 f dp, \quad (4)$$

$$N_2 = N_1 - \frac{d_q V_d}{(2\pi)^3} \int_{\mu_q - \Delta}^{\mu_q} 4\pi p^2 f dp, \quad (5)$$

$$N_3 = N_1 - N_2, \quad (6)$$

where $f = [\exp \beta(p - \mu_q) + 1]^{-1}$ with $\beta = 1/(kT)$. The corresponding energies $E_{1,2,3}$ are

$$E_1 = \frac{d_q V_d}{(2\pi)^3} \int_0^\infty 4\pi p^3 f dp, \quad (7)$$

$$E_2 = E_1 - \frac{d_q V_d}{(2\pi)^3} \int_{\mu_q - \Delta}^{\mu_q} 4\pi p^3 f dp, \quad (8)$$

$$E_3 = \left(\frac{N_3}{2}\right) \left(\frac{\pi}{R_d} - \Delta\right). \quad (9)$$

In the last equation $(N_3/2)$ is the number of Cooper pairs (bosons) in the droplet and (π/R_d) is the energy of the ground state of the single-particle spectrum of a spherical cavity of radius R_d . Due to the small size of the droplet, even the lowest excited state has energy which is very large compared to the temperature. Therefore all the qq pairs tend to occupy the ground state [6]. Next, entropies $S_{1,2,3}$ are given by

$$S_1 = -\frac{d_q V_d}{(2\pi)^3} \int_0^\infty 4\pi p^2 dp [f \ln f + (1 - f) \ln(1 - f)], \quad (10)$$

$$S_2 = S_1 + \frac{d_q V_d}{(2\pi)^3} \int_{\mu_q - \Delta}^{\mu_q} 4\pi p^2 dp [f \ln f + (1 - f) \ln(1 - f)], \quad (11)$$

$$S_3 = 0. \quad (12)$$

S_3 can be taken to be zero for the reasons given above. Finally, the pressures $P_{1,2,3}$ are calculated as follows:

$$P_1 = E_1/(3V_d). \quad (13)$$

The thermodynamic potential Ω for massless quarks is given by

$$\Omega = -kT \sum \ln [1 + \exp \beta(\mu_q - p)].$$

Hence

$$\begin{aligned} P_2 &= -\frac{\Omega}{V_d} = \frac{kTd_q}{(2\pi)^3} \left(\int_0^\infty - \int_{\mu_q - \Delta}^{\mu_q} \right) 4\pi p^2 dp \ln [1 + \exp \beta(\mu_q - p)] \\ &= \frac{E_1}{3V_d} - \frac{kTd_q}{2\pi^2} \int_{\mu_q - \Delta}^{\mu_q} p^2 dp \ln [1 + \exp \beta(\mu_q - p)]. \end{aligned}$$

Performing the last integration by parts and rearranging the terms, one finally gets

$$P_2 = \frac{E_2}{3V_d} - \frac{kTd_q}{6\pi^2} \{ \mu_q^3 \ln 2 - (\mu_q - \Delta)^3 \ln [1 + \exp(\beta\Delta)] \}. \quad (14)$$

The quantal pressure P_3 is given by

$$P_3 = -(\partial E_3 / \partial V_d)_{N_3} = N_3 / 8R_d^4. \quad (15)$$

It is easy to verify that if Δ is set equal to zero, i.e. if no pairing is allowed to take place, N_3 , E_3 , P_3 vanish and N_2 , E_2 , S_2 , P_2 become equal to N_1 , E_1 , S_1 , P_1 , respectively. Contribution of antiquarks to the above thermodynamic quantities is smaller by many orders of magnitude. Although we have included it in our calculations its effect is negligible.

The droplet pressure P_d is given by

$$P_d = P_2 + P_3 + \bar{P}_2 + \bar{P}_3 + P_{gluons}, \quad (16)$$

where P_2 and P_3 are as in Eqs. (14)-(15), \bar{P}_2 and \bar{P}_3 are the corresponding pressures due to antiquarks and P_{gluons} is the pressure due to gluons in the droplet.

Consider once again the spherical region of radius R_d . Initially, i.e. before the pairing interaction is switched on, there are N_1 quarks, \bar{N}_1 antiquarks and a certain number of gluons in it. In the final state, i.e. when the pairing interaction is on, there are N_2 quarks, $(N_3/2)$ quark pairs, \bar{N}_2 antiquarks, $(\bar{N}_3/2)$ antiquark pairs and the same number of gluons

as before. The activation energy (A) is defined as the difference between the Helmholtz free energies (F) in the final and initial states. Since the gluonic contribution cancels out, one gets

$$\begin{aligned} A &= F(N_2) + F(N_3/2) - F(N_1) + F(\bar{N}_2) + F(\bar{N}_3/2) - F(\bar{N}_1) \\ &= E_2 - TS_2 + E_3 - E_1 + TS_1 + \bar{E}_2 - T\bar{S}_2 + \bar{E}_3 - \bar{E}_1 + T\bar{S}_1. \end{aligned} \quad (17)$$

In the limit $\Delta \rightarrow 0$, this A vanishes.

The reader may wonder why surface tension of the droplet makes no appearance in our formalism. In the classical theory of nucleation, there are two competing contributions to the energy of a droplet: droplet formation reduces bulk free energy but only at the cost of surface energy. The former contribution wins if the droplet radius exceeds a certain critical value, while the surface tension ensures that a droplet with a smaller radius shrinks and disappears. In the formalism presented here, energy of the droplet is calculated quantum mechanically. It is clear from Eq. (9) that small droplets have large quantal energy and tend to dissolve back into the QGP gas. This is similar to the effect of the surface tension in the classical theory. Moreover, the thermal wavelength (λ) of the quarks is so large that a classification of particles as those localized on the surface and those in the interior breaks down. In short, we did not neglect the surface energy; it is included in the total free energy of the quantal droplet.

III. RESULTS AND DISCUSSION

The precise boundaries of the various phases in Fig. 1 are not known. Since the baryon number density (n_B) of the normal nuclear matter is $\sim 0.17 \text{ fm}^{-3}$, we have performed numerical calculations for $n_B = 0.5$ to 3 fm^{-3} and temperature $T = 0$ to 100 MeV . The resulting quark chemical potential μ_q varies over $\sim 250 - 600 \text{ MeV}$ and the baryon chemical potential¹

¹This definition is applicable only for a gas of quarks, and not for the normal nuclear matter.

$\mu_B \equiv 3\mu_q$ varies over $\sim 750 - 1800$ MeV. This fully covers the densities likely to be seen in the neutron-star cores. We have considered four different values of the superconducting gap parameter Δ , namely, 1, 10, 50 and 100 MeV.

Since we are interested in a gas of weakly interacting quarks, antiquarks and gluons, we take α_s to be zero. Small values of α_s do not affect the results in Eqs. (1)-(3) significantly. We first choose a set of values for n_B and T , and solve Eq. (1) numerically to determine μ_q . This μ_q is then used to evaluate P_{gas} as given by Eq. (3). Also, once μ_q is determined, n_q and $n_{\bar{q}}$ can be evaluated separately by using

$$n_q = \frac{d_q}{(2\pi)^3} \int_0^\infty 4\pi p^2 f dp,$$

$$n_{\bar{q}} = n_q(\mu_q \rightarrow -\mu_q)$$

(Above integrations cannot be done analytically, and so it is not possible to get closed expressions like Eq. (1), for n_q and $n_{\bar{q}}$.) Next, we choose a value for Δ , and treating the droplet radius R_d as a free parameter, calculate various other quantities; see Eqs. (4)-(17). Some of these results are shown in Figs. 3-4.

In our formalism, as in the classical theory, the activation energy when plotted as a function of the radius (Fig. 3), initially increases from zero, attains a maximum, then starts decreasing monotonically eventually becoming negative for a sufficiently large value of the radius. In other words, the activation energy exhibits a barrier. *The barrier originates as follows.* Consider Eq. (17). As already stated, the antiquark terms are extremely small. The terms TS_1 and TS_2 are also negligible and in fact they tend to cancel each other. That leaves three terms, namely E_1 , E_2 and E_3 . For small radii, E_2 and the quantal energy term E_3 dominate pushing the activation energy curve upwards. For large radii, the E_1 term dominates pulling the curve to the negative domain. As expected, the barrier becomes wider if T is raised or if n_B is lowered. The critical radii can be read off from Fig. 3. Droplets with larger radii readily grow because that tends to reduce the activation energy. This in turn easily brings about the transition from QGP to the superconducting phase.

Figure 4 shows the ratio of the droplet pressure to the pressure of the surrounding gas,

for $\Delta = 100$ MeV. This ratio is significantly larger than unity for small droplets, which will tend to push the radii to larger values, thereby helping to bring about the QGP to superconducting phase transition. In the limit $\Delta \rightarrow 0$, this ratio tends to unity and is thus incapable of pushing the droplet radii to larger values.

It is interesting to know the properties of the droplet when the pressure inside the droplet (Eq. 16) equals the pressure of the surrounding QGP gas (Eq. 3). These results are shown in Figs. 5-8. The condition $P_d = P_{gas}$ fixes R_d . We solve the equation $P_d = P_{gas}$ numerically to determine R_d , for various values of n_B , T and Δ . n_B was varied from 0.5 to 3 fm⁻³ in the steps of 0.5 fm⁻³. Figure 5 shows the results for R_d . As T and/or n_B are increased, R_d decreases. However, R_d is found to be rather insensitive to the variation in n_B . Although we have varied T between 0 and 100 MeV, temperatures relevant for neutron stars are close to zero. Because of the small value of R_d , the energy of even the lowest excited state inside the droplet turns out to be several hundreds of MeV which is large compared to the temperature, effectively forcing all Cooper pairs (bosons) to occupy the ground state. *Note also that at low temperatures, the droplet radius R_d is larger than the Pippard coherence length $\xi \simeq 1/(\pi\Delta)$.*

Figure 6 shows the activation energy A . First see the upper half of Fig. 6. For a fixed n_B , as T increases, A changes its sign from negative to positive. This is expected because, at higher T , droplet formation is energetically unfavourable. Secondly, as n_B increases (see curves labelled a to f), A remains negative up to higher and higher T . This is also expected because at higher n_B , the transition to the superconducting phase is facilitated. Now see the lower half of Fig. 6. It shows the $A = 0$ contour, in the $T - n_B$ plane. This is also the phase transition curve separating the QGP phase at high T and the superconducting phase at low T : Recall $A \equiv F_{SC} - F_{QGP}$ where F are the free energies of the two phases. Both F_{SC} and F_{QGP} decrease as T increases and cross each other at some temperature, say T_c (Fig. 7). Since the system follows the path of minimum F , there is a kink in $F(T)$. In other words, the slope $dF/dT = -S$ has a discontinuity, indicating a first-order phase transition at T_c . Thus the $A = 0$ contour serves to demarcate the region of the superconducting phase. Note that as n_B increases, the $A < 0$ region in Fig. 6 survives up to higher and higher T .

We now present an estimate of the latent heat (L) associated with the first-order phase transition considered in this paper. The transition temperature T_c for any given n_B can be determined from Fig. 6. The latent heat is then estimated as $L = T_c \times (S_1(T_c) - S_2(T_c))$. For $\Delta = 100$ MeV, this turns out to be ~ 150 to ~ 250 MeV and it increases with n_B . In the limit $\Delta \rightarrow 0$, the two free-energy curves in Fig. 7 coincide, A vanishes, $S_1 = S_2$, there is no discontinuity in entropy, and the latent heat is zero. There is only one phase namely QGP, and there is no question of any phase transition.

Finally, Fig. 8 shows 3-dimensional surface plots of the (normalized) activation energy A' defined as $A' \equiv (F_{SC} - F_{QGP})/(F_{SC} + F_{QGP})$ as a function of n_B and T , for $\Delta = 1$ and 100 MeV. It is clear that in the limit $\Delta \rightarrow 0$, the activation energy surface is flat and there is no energy advantage for the QGP to superconducting phase transition. Indeed there would be only one phase, namely QGP, which would extend up to the $T = 0$ axis. On the other hand, for $\Delta = 100$ MeV, the surface is such that the system would like to “roll down” the slope thereby bringing about the phase transition.

It is interesting to compare the activation energy results for the QCD phase transition, obtained here with those for the Bose-Einstein condensation in a gas of trapped atomic hydrogen, presented in [6]. In [6] two gas densities were considered: 10^{14} cm^{-3} and $7 \times 10^{13} \text{ cm}^{-3}$ both at the same temperature $50 \mu K$. We have repeated their calculations for $T = 45 - 55 \mu K$. Their activation energy exhibits a barrier, and they denote the maximum value of the activation energy by A_0 . Consider the ratio A_0/kT at the peak position and the corresponding number \tilde{N}_0 of particles in the droplet. In [6] these two quantities are highly sensitive to the changes in the gas density and temperature.² For instance, for the above tiny change in the gas density, the ratio A_0/kT changes from 4.8 to 104.1, and \tilde{N}_0 changes from 18 to 3862. Similar sensitivity was seen when T was changed by a few μK . In contrast,

²There is a misprint in [6]: in Fig. 1, the y-axis label should read $A(10^{-10})$ a.u. For the inset, it is $A(10^{-8})$ a.u.

the results presented here are relatively stable with respect to changes in n_B and T .

In conclusion, we have studied hitherto unexplored first-order phase transition from QGP to a colour-superconducting phase, and have presented a simple model of the transition with very few assumptions. It provides numerical support to the prevalent ideas of phase structure of QCD in the low-temperature, high-baryon-number-density regime. We have studied properties of the droplets of the superconducting phase, formed at various points in the $T - n_B$ plane, for several values of the gap parameter. We have been able to estimate the extent of the superconducting phase in this plane and the latent heat of the transition. At low temperatures, droplet radii are found to be larger than the Pippard coherence length which measures the spatial extent of the qq Cooper pairs.

RSB acknowledges the hospitality of the McMaster University where this work was initiated. We thank Mark Alford and Mustansir Barma for their comments on this work. This research was partially supported by a grant from NSERC (Canada).

Appendix

If $f(p)$ is the distribution function of a gas in equilibrium, the number density n is given by $n = \int f(p) d^3p / (2\pi\hbar)^3$. For a nonrelativistic classical gas at temperature T , one has

$$f = \exp \left[-\beta \left(\frac{p^2}{2m} - \mu \right) \right],$$

where $\beta = 1/kT$ and μ is the chemical potential. Hence

$$n = \exp(\beta\mu) (2\pi\hbar^2/mkT)^{-3/2} \equiv \exp(\beta\mu) \lambda^{-3},$$

where λ is the thermal wave length.

For an extreme relativistic gas of massless classical particles,

$$f = \exp [-\beta(pc - \mu)],$$

and hence

$$n = \exp(\beta\mu) (c\hbar\pi^{2/3}/kT)^{-3}.$$

We define the thermal wave length in this case as $\lambda = c\hbar\pi^{2/3}/kT$, so that the fugacity $\exp(\beta\mu)$ once again equals $n\lambda^3$.

REFERENCES

- [1] K. Rajagopal and F. Wilczek in *Handbook of QCD*, M. Shifman, ed., pp. 2061-2151 (World Scientific, 2001), e-print hep-ph/0011333.
- [2] T. Schäfer and E.V. Shuryak, Lect. Notes Phys. 578 (2001) 203, e-print nucl-th/0010049.
- [3] M. Alford, Ann. Rev. Nucl. Part. Sci. 51 (2001) 131, e-print hep-ph/0102047.
- [4] K. Rajagopal, private communication.
- [5] See, for example, M.A. Preston and R.K. Bhaduri, *Structure of the Nucleus*, (Addison-Wesley, Reading, MA, 1975).
- [6] R. Côté and V. Kharchenko, Phys. Rev. Lett. 83 (1999) 2100.
- [7] M. Alford, K. Rajagopal and F. Wilczek, Phys. Lett. B 422 (1998) 247.
- [8] G. Neergaard and J. Madsen, Phys. Rev. D 62 (2000) 034005.
- [9] B. Müller, *The Physics of the Quark-Gluon Plasma*, Lecture Notes in Physics, vol. 225, (Springer-Verlag, Berlin, 1985).
- [10] B.O. Kerbikov, e-print hep-ph/0110197.

FIGURE CAPTIONS

FIG. 1. Schematic phase diagrams of QCD: T is the temperature and μ_B is the baryon chemical potential. E is the critical point at which the line of first-order phase transitions ends. $2SC$ and CFL (Colour-Flavour-Locked) are 2-flavour-like and 3-flavour-like colour superconducting phases, respectively. The dashed line denotes the critical temperature at which quark-quark pairing vanishes. The thick arrow indicates the first-order phase transition considered in this paper. For the normal nuclear matter at $T = 0$, μ_B should be defined as $m_N + \hbar^2 k_F^2 / 2m_N$ where $k_F \simeq 1.4 \text{ fm}^{-1}$ [5] and m_N is the nucleon mass, which gives $\mu_B \simeq 980 \text{ MeV}$. (Figure adapted from [1].)

FIG. 2. Feynman diagrams contributing to the equation of state of quark-gluon plasma in order α_s . Curly lines: gluons, dashed lines: ghost particles, solid lines: quarks.

FIG. 3. Activation energy A vs droplet radius R_d for various gap values Δ . Baryon number density n_B (fm^{-3}) and temperature T (MeV) are: (a) 0.5 and 5 (b) 0.5 and 100 (c) 3 and 5 (d) 3 and 100, respectively.

FIG. 4. Ratio of the pressure of the droplet to the pressure of the surrounding QGP gas vs droplet radius R_d , at gap $\Delta = 100 \text{ MeV}$. Curve labels are as in Fig. 3.

FIG. 5. Droplet radius R_d vs temperature T for various gap values Δ . Results are insensitive to n_B , so not all curves are labelled.

FIG. 6. Upper panel: Activation energy A vs temperature T . Baryon number densities n_B (fm^{-3}) are (a) 0.5 (b) 1 (c) 1.5 (d) 2 (e) 2.5 (f) 3. Lower panel: The $A = 0$ contour or the phase transition line in the $T - n_B$ plane. SC: superconducting phase.

FIG. 7. Free energies F_{QGP} and F_{SC} in the QGP and superconducting phases, respectively, vs temperature T .

FIG. 8. Three-dimensional surface plots of the activation energy A' for $\Delta = 1 \text{ MeV}$ (upper part) and $\Delta = 100 \text{ MeV}$ (lower part), as a function of n_B (fm^{-3}) and T (MeV).

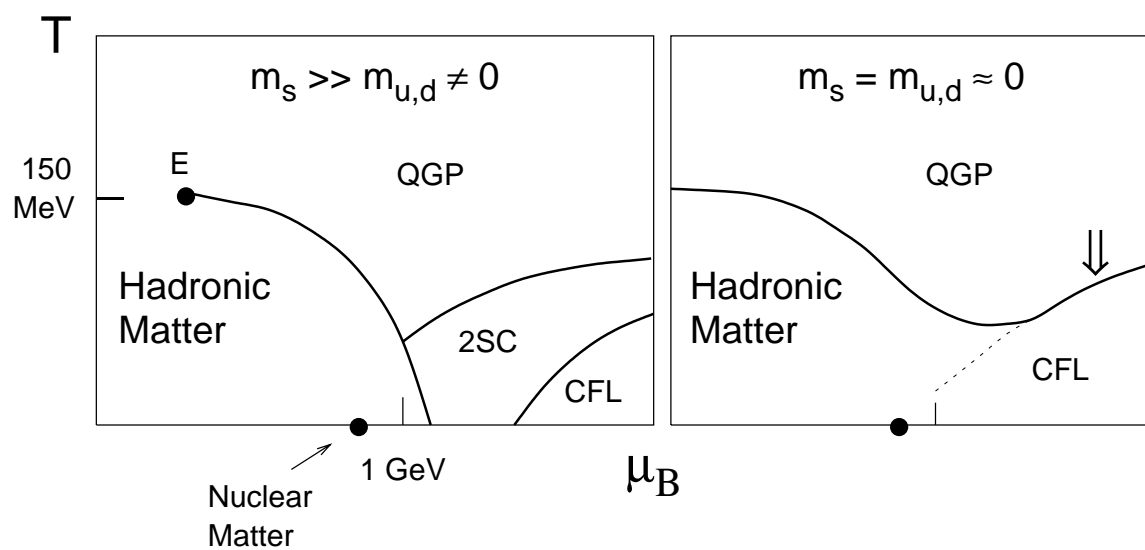


FIG. 1.

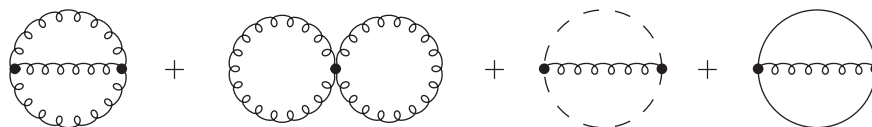


FIG. 2.

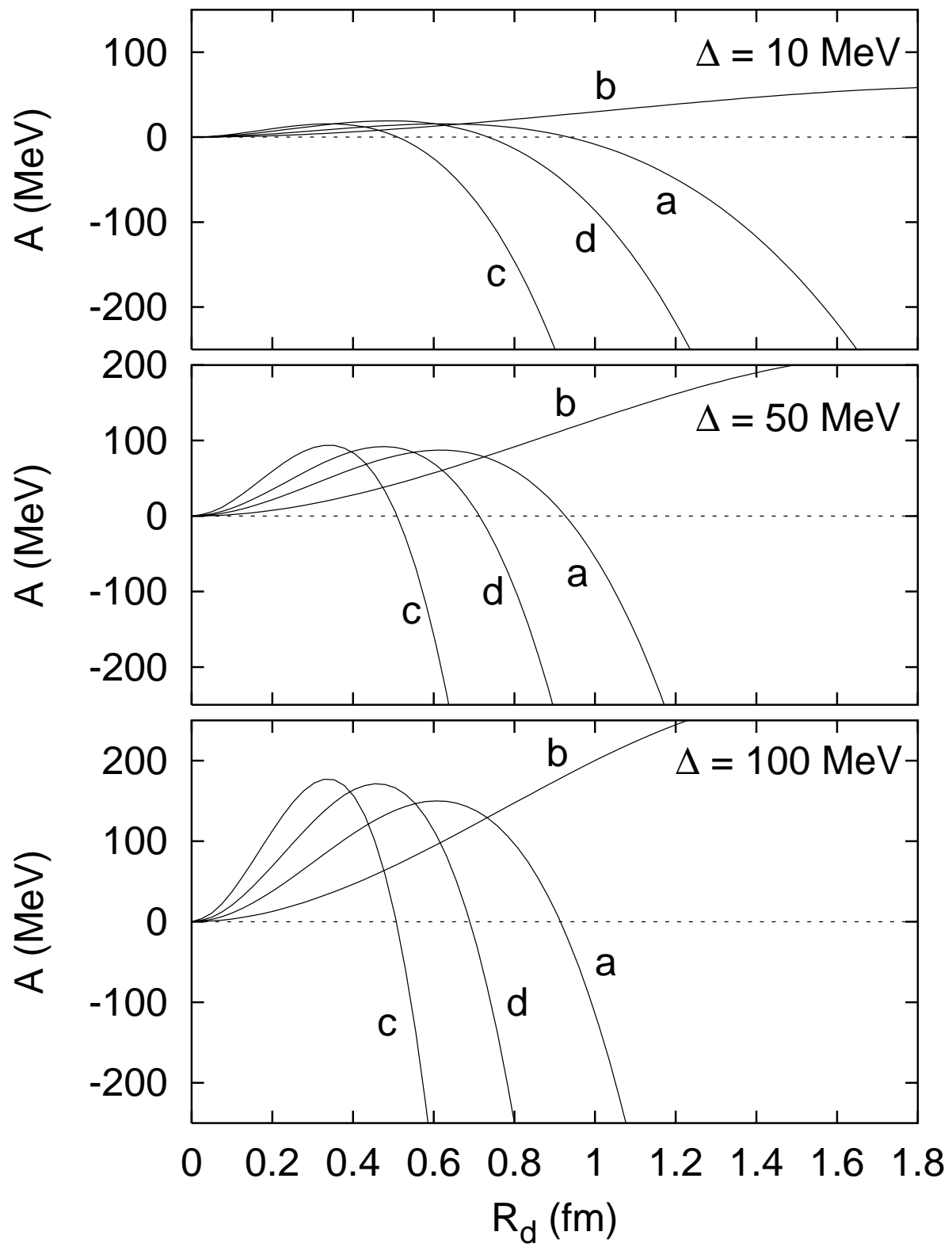


FIG. 3.

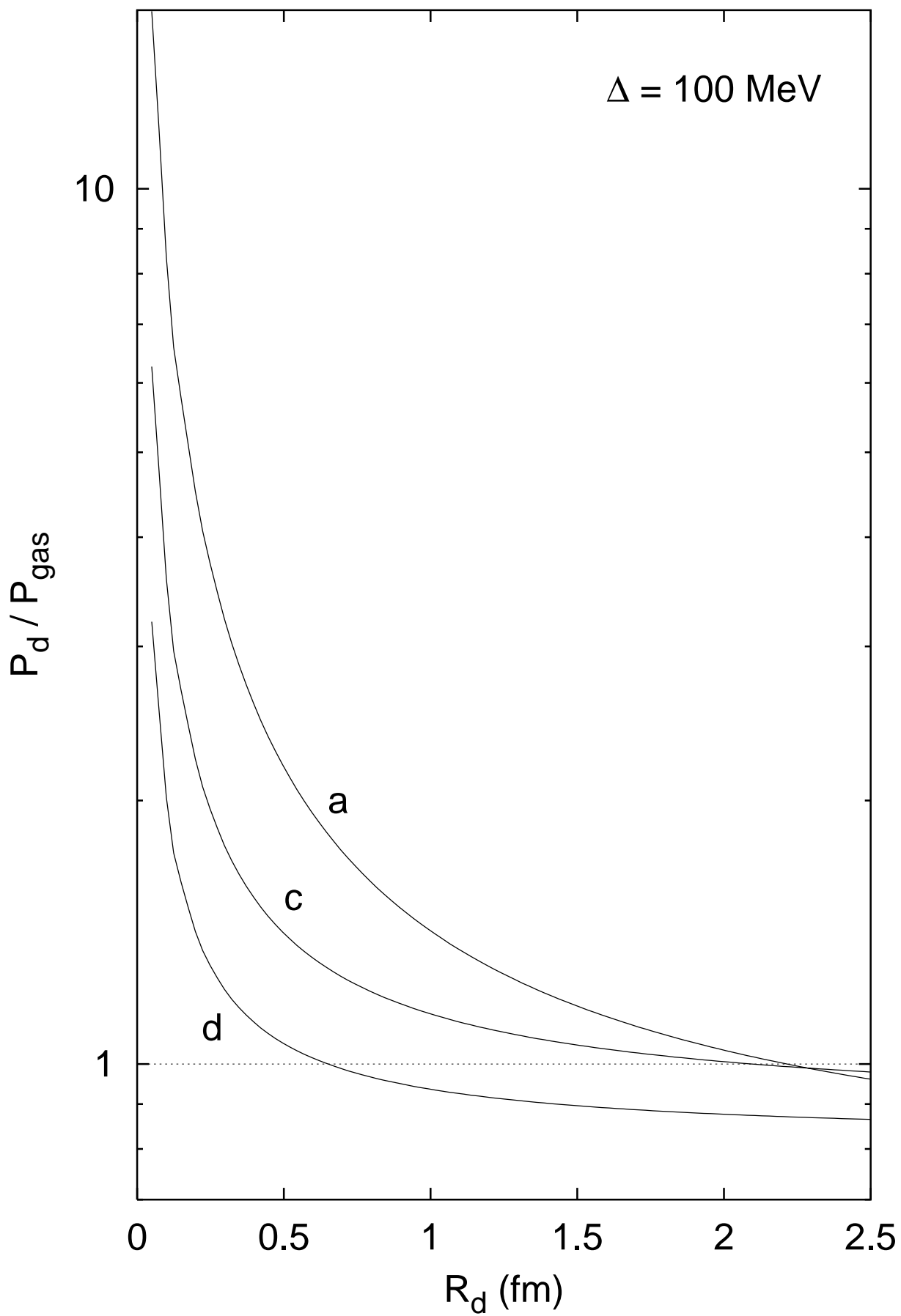


FIG. 4

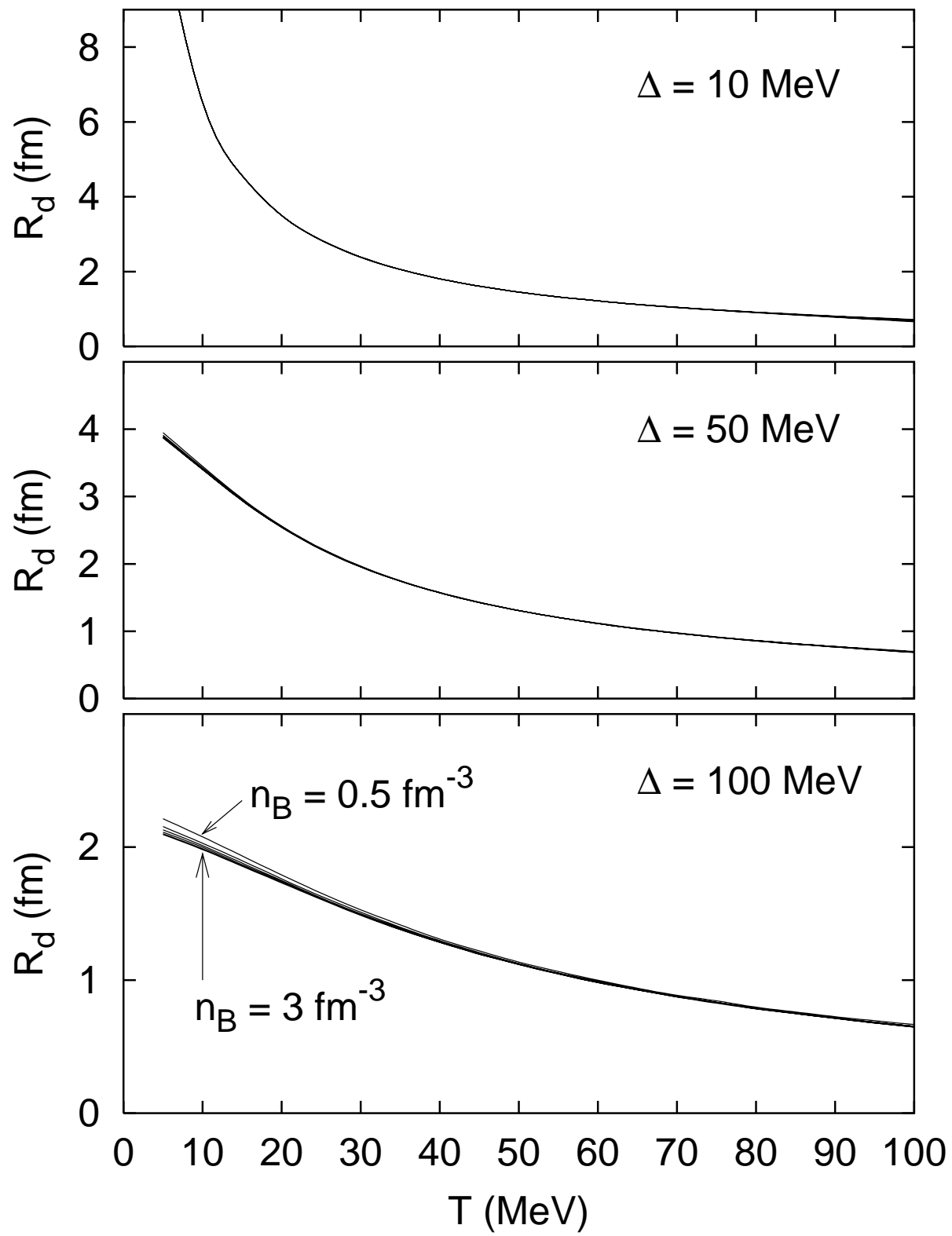


FIG. 5.

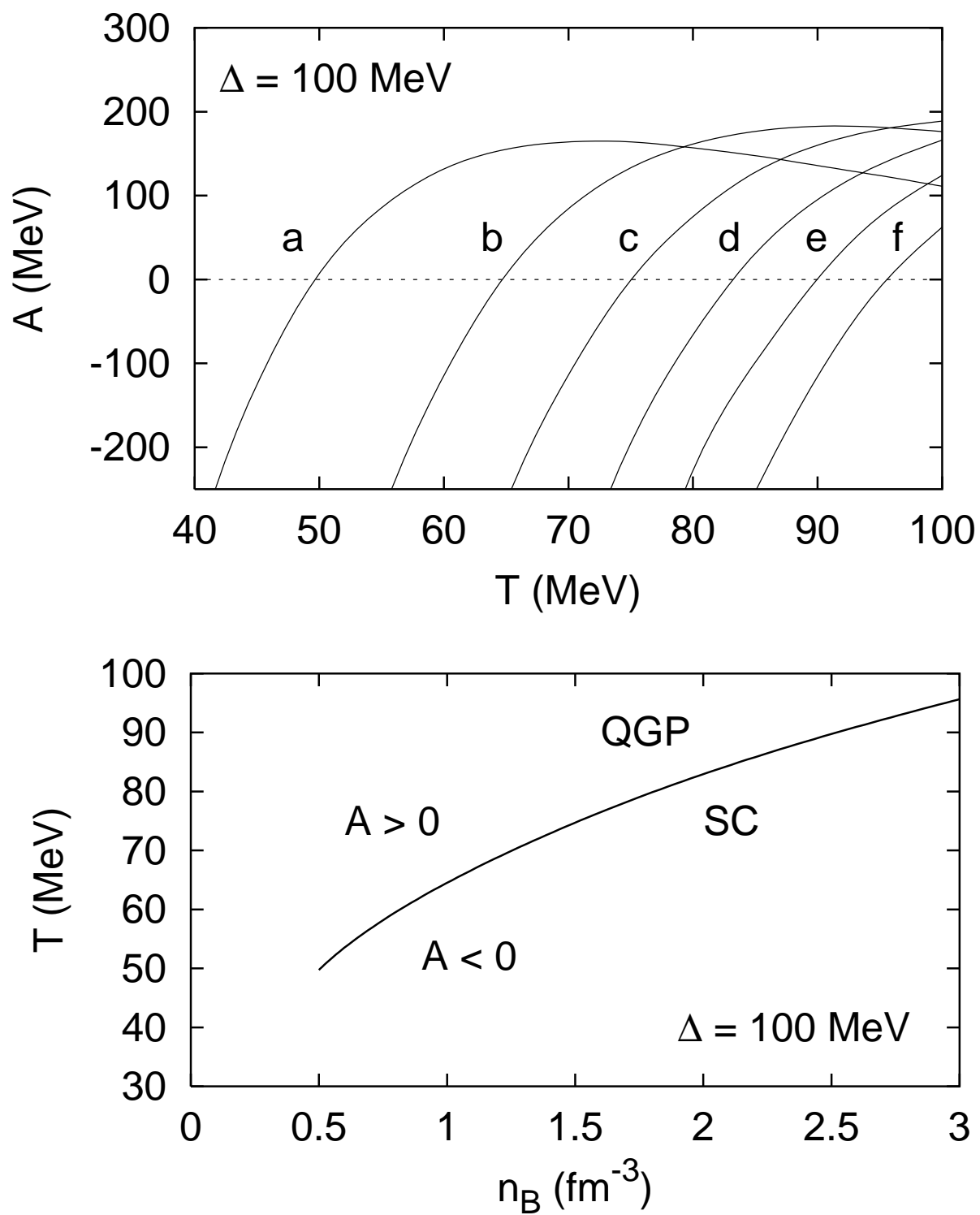


FIG. 6.

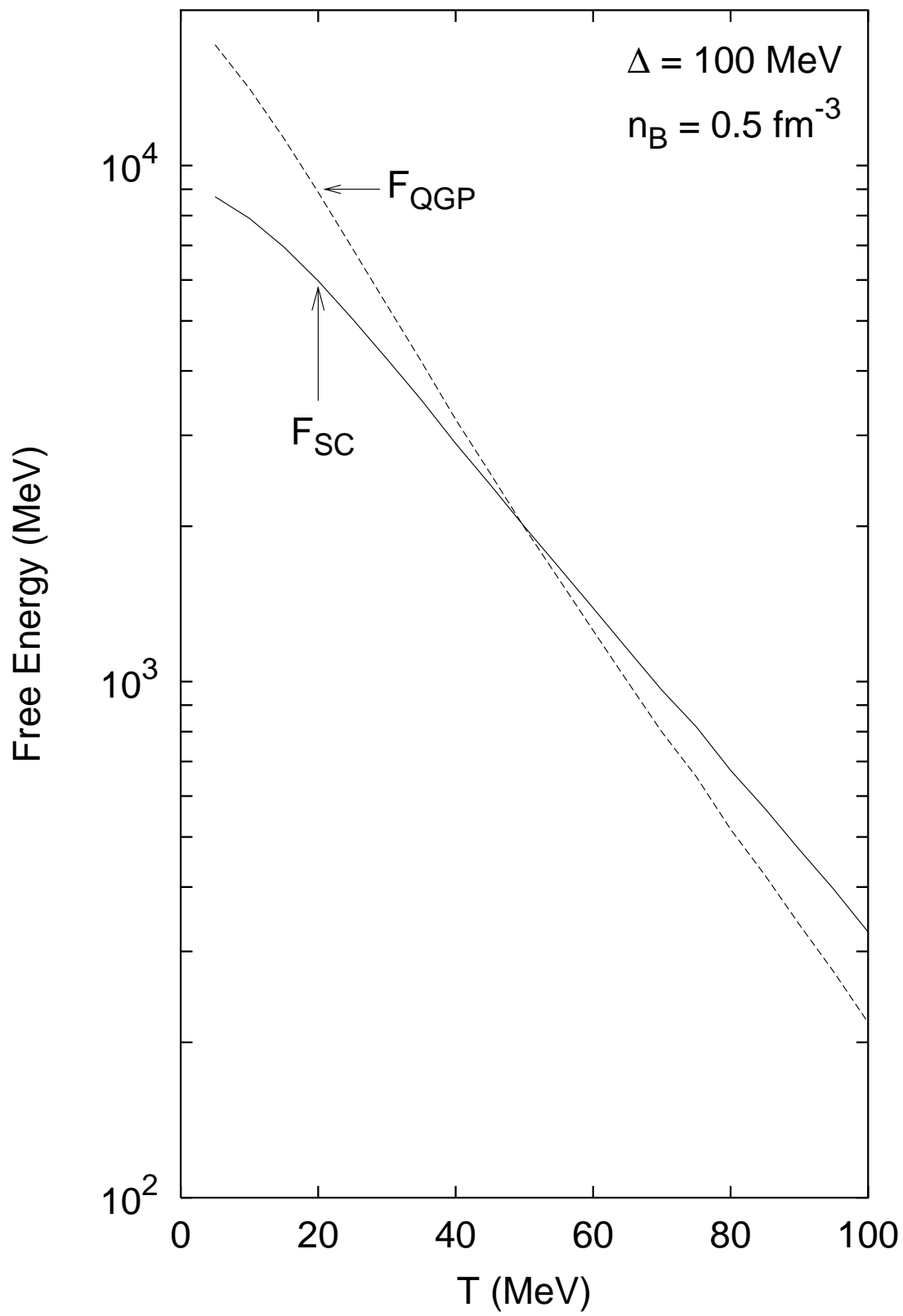


FIG. 7.

